

Article

Not peer-reviewed version

Quasi-Analytical Solution of Kepler's Equation as an Explicit Function of Time

A.N. Beloiarov , V.A. Beloiarov , [Raúl C. Cruz-Gómez](#) ^{*} , C. O. Monzón , [J.L. Romero](#)

Posted Date: 15 May 2024

doi: 10.20944/preprints202405.1019.v1

Keywords: Kepler's equation; quasi-analytical solution; celestial bodies; Kepler's laws



Preprints.org is a free multidiscipline platform providing preprint service that is dedicated to making early versions of research outputs permanently available and citable. Preprints posted at Preprints.org appear in Web of Science, Crossref, Google Scholar, Scilit, Europe PMC.

Copyright: This is an open access article distributed under the Creative Commons Attribution License which permits unrestricted use, distribution, and reproduction in any medium, provided the original work is properly cited.

Article

Quasi-Analytical Solution of Kepler's Equation as an Explicit Function of Time

A.N. Beloiarov, V.A. Beloiarov, R.C. Cruz-Gómez *, C.O. Monzón and J.L. Romero

Departamento de Física, Universidad de Guadalajara, Blvd. Marcelino García Barragán y Calzada Olímpica, Guadalajara, 44840, Jalisco, México; viacheslav.beloiarov2962@alumnos.udg.mx; sbeloiarov@lincolnschool.edu.mx; jose.ribarra@academicos.udg.mx; cesar.monzon@academicos.udg.mx

* Correspondence: raul.cruz@academicos.udg.mx

Abstract: Although the empirical Kepler's laws can be proven by applying Newton's laws to the dynamics of two particles attracted due to the gravitational interaction, there is no explicit formula for the motion as a function of time. In this paper, a quasi-analytical solution for this problem is proposed. It approximates the real behavior of celestial bodies with an acceptable degree of accuracy. All calculations involved require a low computational cost. This problem is closely related to Kepler's equation, since, the solution for the equations of motion as a function of time gives us the solution to Kepler's equation as well. The results are presented for each planet of the solar system (including Pluto), and the solution is compared against the real orbits.

Keywords: Kepler's equation; quasi-analytical solution; celestial bodies; Kepler's laws

1. Introduction

Kepler's laws provide an empirical mathematical model to describe the dynamics of the motion of the planets around the Sun (later proven by Newton's analytical results [1,2]. Therefore, they are of fundamental importance in astrophysics, celestial mechanics, and earth science [3]. In this way and under the Copernican hypothesis, where the Earth rotates on itself and around the Sun, phenomena such as the apparent motion of the stars and the flattening of the Earth, among others, could be explained. Nevertheless, Kepler's fundamental problem is the motion of a planet over time as it traverses through its orbit. As we shall see, it is the so-called Kepler's equation (KE) that provides the explicit time dependence of the fundamental quantities of the problem. Since this equation was first established by Kepler in 1609, until the present day, several solutions of different types have been proposed [2,4–6]. Due to its inherent nature, it has not yet been possible to obtain an exact explicit solution, and a large number of calculations must be made to improve the approximate solutions. It is hardly possible to refer here to all the relevant works. Some of the procedures give satisfactory approximations, but they are very complex and often require many terms in order to obtain a solution with a given degree of accuracy and may involve high computational cost [3,7]. These solutions normally consist of calculating infinite series, or high-order iterative approaches [3,7–10,12,14] and by integral solutions [13]. Recently, some methods which use artificial intelligence were proposed [11].

In this work, we present a quasi-analytical solution that gives the explicit equations of motion as a function of time. This solution is quasi-analytical because even though it gives explicit formulas, it depends on six numerical coefficients, which in turn depend on the eccentricity. As mentioned above, this result provides an explicit solution to KE.

1.1. The Orbit Equation

The classical problem begins then, with the description of the motion of the planets according to the following equations [15]:

$$t(\theta) = \frac{a^2 \mu}{l} \int_0^\theta \frac{1}{(1 + \varepsilon \cos \varphi)^2} d\varphi, \quad (1)$$

where

$$r(\theta) = \frac{\alpha}{1 + \varepsilon \cos \theta}, \quad (2)$$

has been used. Here, (r, θ) are the coordinates of the planet in the polar coordinate system, with the origin at the Sun, t is the time, ε is the eccentricity, and a , μ , and l are the focal parameter, the reduced mass, and the angular momentum, respectively [2]. The angle θ is called *the true anomaly*, defined as $\theta = 0$ at the pericenter [14].

The inverse of the solution of Eq. (1), $\theta(t)$ is closely related to KE:

$$E - \varepsilon \sin E = M, \quad (3)$$

where E is the *eccentric anomaly* and M is the *mean anomaly*, expressed as:

$$M = \frac{2\pi}{T} t, t \in [0, T], \quad (4)$$

T being the orbital period. As was pointed out before, usually, E needs to be estimated by series expansions [16] or iterative methods [6]. Thus, the accuracy of the position and/or velocity of the celestial object moving in the Keplerian orbit, which may be obtained from the solution of KE, depends on the approximation method used. Figure 1 illustrates the variables involved in the problem.

Equations (1) and (3) are both transcendental. The solution of Eq. (1) gives the solution of the Eq. (3), and vice-versa, which has led to a vast literature concerning alternative approaches [3]. A detailed description of the different works presented in the literature on this problem can be found in [3,14].

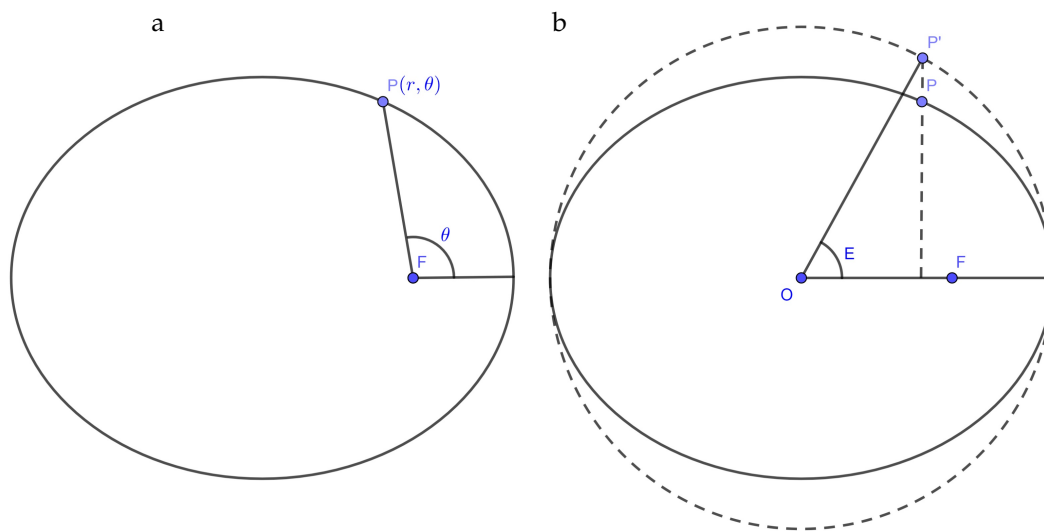


Figure 1. Illustration of the relative position of the Sun and planet (a) and Kepler's equation (b).

The remainder of this paper is structured as follows. In Section 2 we present in detail, step by step, the quasi-analytical solution of Eq. (1). In Section 3 the results are presented and compared with the real orbit of each planet of the solar system. In Section 4 we present the solution to KE based on the solution of Eq. (1). Finally, in Section 5 we give a brief discussion and conclusions about the results obtained in this work.

2. Methodology

In the present section, the quasi-analytical method is established for solving Eq. (1). For clarity, we divide the method into sections that we will call steps. All calculations and graphics were performed with MATLAB 2020b. Now we briefly describe each step.

Step 0. In this step we integrate Eq. (1) and introduce a normalized time τ which maps the real time t from the interval $[0, T]$ to the interval $[0, \pi]$, which leads us to Eq. (7) for $\tau(\theta)$.

Step 1. In this step we separate $\tau(\theta)$ into two parts, $\tau_a(\theta)$ and $\tau_b(\theta)$. Based on the observation that $\tau_a(\theta)$ resembles the behavior of $\tau(\theta)$ (especially for small values of ε), and, taking into account its analytical form, we find the inverse of $\tau_a(\theta)$, $\theta_0(\tau)$ as our zeroth approximation for $\theta(\tau)$.

Step 2. Assuming the exact solution has the form of Eq. (14), we introduce the *true* argument of the arctangent function, $\varphi(\tau)$, which gives the exact solution. Then, we introduce the function $\psi_0(\tau)$ (Eq. (17)) as the quotient of the *true* argument $\varphi(\tau)$ and the argument of the zeroth approximation, $\varphi_0(\tau)$. Finally, we define the first approximation $\theta_1(\tau)$ by adjusting the argument $\varphi_0(\tau)$ of the arctangent function which appears in the zeroth approximation $\theta_0(\tau)$. The main idea is to make a series of adjustments in such a way that the quotient mentioned above approaches 1 as closely as possible.

Step 3. Following the logic of *Step 2*, we introduce the function $\psi_1(\tau)$ (Eq. (22)) and the argument $\varphi_2(\tau)$ (Eq. (25)) in order to obtain the second approximation $\theta_2(\tau)$ (Eq. (26)). First, we propose two kinds of approximations for $\psi_1(\tau)$: linear and harmonic. This gives the approximations $\theta_{2.1}(\tau)$ and $\theta_{2.2}(\tau)$ (Eqs. (27) and (28)), respectively. This approximations give the corresponding precision of 3,400 km and 470 km, respectively, for the position of the Earth. This formulas are completely analytical, and may be used in some applications which do not require high precision.

Next, we proceed to improve the function $\psi_1(\tau)$ as an analytical expression (Eq. (29)), involving an arctangent function, with an argument which, in turn, is an expression that depends on six numerical coefficients (Eq. (30)). In order to calculate these coefficients, we propose two methods, namely, *Method A* and *Method B*.

Method A consists in calculating the coefficients for fixed values of the eccentricity, while *Method B* allows us to express these coefficients as an analytic function with other numeric coefficients calculated for ranges of the eccentricity.

2.1. Step 0

Our first step is integrating Eq. (1) to obtain $t(\theta)$. The solution is (see Appendix A):

$$t(\theta) = \frac{\alpha^2 \mu}{l} \left[\frac{2}{(1-\varepsilon^2)^{\frac{3}{2}}} \arctan \left(\sqrt{\frac{1-\varepsilon}{1+\varepsilon}} \tan \frac{\theta}{2} \right) - \frac{2\varepsilon}{1-\varepsilon^2} \frac{\tan \frac{\theta}{2}}{1+\varepsilon+(1-\varepsilon) \tan^2 \frac{\theta}{2}} \right]. \quad (5)$$

This solution is valid on the interval $\theta \in [-\pi, \pi]$. In order to make the solution valid on the interval $\theta \in (-\infty, \infty)$, we need to apply the following correction:

$$t_1(\theta) = 2t(\pi) \left\lfloor \frac{(1+(\theta-\pi))}{2\pi} \right\rfloor + t(\theta). \quad (5a)$$

In order to avoid complications related with the periodicity of the functions of θ involved, and the monotony of time, in what follows, we focus our work only on the half-period of the orbit, namely, $\theta \in [0, \pi]$. The second half of the orbit may be obtained from the first part using the symmetry of the orbit.

We now propose the following change of variable:

$$\tau = \frac{l}{\alpha^2 \mu} \frac{(1-\varepsilon^2)^{\frac{3}{2}}}{2} t. \quad (6)$$

So, Eq. (5), in terms of τ and θ has the form:

$$\tau(\theta) = \begin{cases} \arctan \left(\sqrt{\frac{1-\varepsilon}{1+\varepsilon}} \tan \frac{\theta}{2} \right) - \varepsilon \sqrt{1-\varepsilon^2} \frac{\tan \frac{\theta}{2}}{1+\varepsilon+(1-\varepsilon) \tan^2 \frac{\theta}{2}}, & \theta \in [0, \pi), \\ \frac{\pi}{2}, & \theta = \pi. \end{cases} \quad (7)$$

Let us seek for the solution to Eq. (7) in the form $\theta(\tau)$ on the interval $\theta \in [0, \pi]$, and, as deduced from Eq. (7), in $\tau \in [0, \frac{\pi}{2}]$.

Note the relationship between τ and the mean anomaly M :

$$\tau = \frac{M}{2}. \quad (8)$$

2.2. Step 1

We rewrite Eq. (7) as follows:

$$\tau(\theta) = \begin{cases} \tau_a(\theta) - \tau_b(\theta), & \theta \in [0, \pi), \\ \frac{\pi}{2}, & \theta = \pi, \end{cases} \quad (9)$$

where:

$$\tau_a(\theta) = \arctan\left(\sqrt{\frac{1-\varepsilon}{1+\varepsilon}} \tan \frac{\theta}{2}\right), \quad (10)$$

$$\tau_b(\theta) = \varepsilon \sqrt{1-\varepsilon^2} \frac{\tan \frac{\theta}{2}}{1 + \varepsilon + (1-\varepsilon) \tan^2 \frac{\theta}{2}}. \quad (11)$$

Figure 2 shows the behavior of $\tau(\theta)$, $\tau_a(\theta)$ and $\tau_b(\theta)$ with ε as parameter.

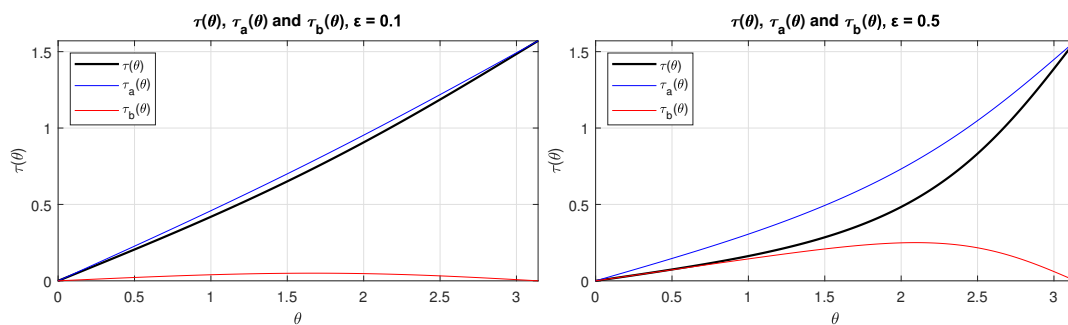


Figure 2. Plots of $\tau(\theta)$, $\tau_a(\theta)$ and $\tau_b(\theta)$ with $\varepsilon = 0.1$ (left) and $\varepsilon = 0.5$ (right).

As we can see, Figure 2 shows how $\tau_a(\theta)$ is similar to $\tau(\theta)$, therefore, as our zeroth approximation $\theta_0(\tau)$, we will solve the following equation:

$$\tau(\theta) = \tau_a(\theta) = \arctan\left(\sqrt{\frac{1-\varepsilon}{1+\varepsilon}} \tan \frac{\theta}{2}\right). \quad (12)$$

To solve the Eq. (12) we apply the tangent function to both parts. Solving for θ , we obtain:

$$\theta_0(\tau) = \begin{cases} 2 \arctan\left(\sqrt{\frac{1+\varepsilon}{1-\varepsilon}} \tan \tau\right) & \tau \in [0, \frac{\pi}{2}), \\ \pi, & \tau = \frac{\pi}{2}. \end{cases} \quad (13)$$

Figure 3 shows plots of $\theta(\tau)$ and $\theta_0(\tau)$ with ε as parameter. $\theta(\tau)$ was obtained using Eq. (7) and interchanging axes.

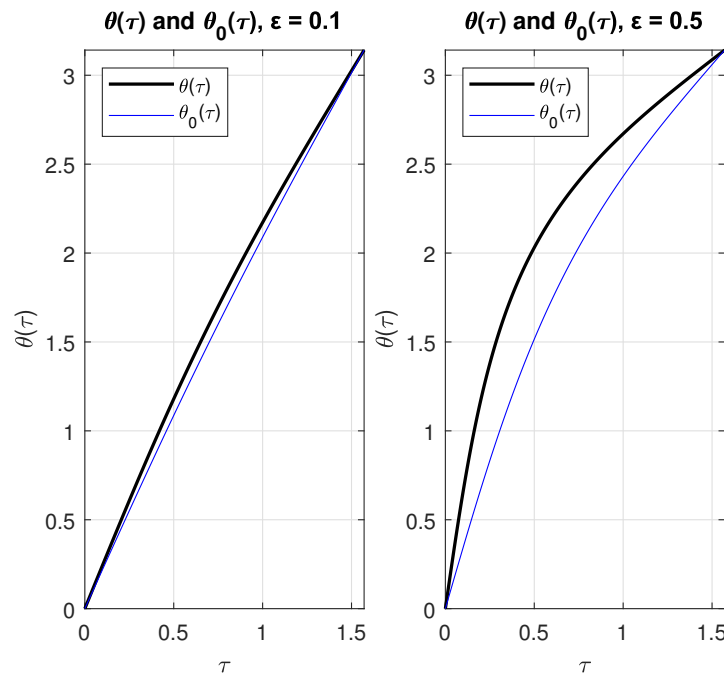


Figure 3. Plots of $\theta(\tau)$ and $\theta_0(\tau)$ with $\varepsilon = 0.1$ (left) y $\varepsilon = 0.5$ (right).

2.3. Step 2

We introduce the functions $\varphi(\tau)$ and $\varphi_0(\tau)$ as follows:

$$\theta(\tau) = 2 \arctan[\varphi(\tau)], \quad (14)$$

$$\varphi_0(\tau) = \sqrt{\frac{1+\varepsilon}{1-\varepsilon}} \tan \tau, \quad (15)$$

so that:

$$\theta_0(\tau) = 2 \arctan[\varphi_0(\tau)]. \quad (16)$$

Now, we introduce another function $\psi_0(\tau)$, defined on the open interval $\tau \in (0, \frac{\pi}{2})$:

$$\psi_0(\tau) = \frac{\varphi(\tau)}{\varphi_0(\tau)}. \quad (17)$$

Appendix B proves the following limits (the former is used immediately to introduce the function $\varphi_1(\tau)$, and the latter is used in step 3):

$$\lim_{\tau \rightarrow 0} \psi_0(\tau) = \frac{1}{1-\varepsilon}, \quad (18)$$

and

$$\lim_{\tau \rightarrow \frac{\pi}{2}} \psi_0(\tau) = 1 + \varepsilon. \quad (19)$$

Now, we introduce, using Eq. (15) and Eq. (18), the function $\varphi_1(\tau)$ as follows:

$$\varphi_1(\tau) = \lim_{\tau \rightarrow 0} \psi_0(\tau) \varphi_0(\tau) = \frac{1}{1-\varepsilon} \varphi_0(\tau) = \frac{\sqrt{1+\varepsilon}}{(1-\varepsilon)^{\frac{3}{2}}} \tan \tau. \quad (20)$$

We define the approximation one, $\theta_1(\tau)$ as follows:

$$\theta_1(\tau) = \begin{cases} 2 \arctan[\varphi_1(\tau)] = 2 \arctan\left(\frac{\sqrt{1+\varepsilon}}{(1-\varepsilon)^{\frac{3}{2}}} \tan \tau\right), \tau \in (0, \frac{\pi}{2}), \\ 0, \tau = 0, \\ \pi, \tau = \frac{\pi}{2}. \end{cases} \quad (21)$$

Figure 4 shows plots of $\theta(\tau)$ and $\theta_1(\tau)$ with ε as parameter.

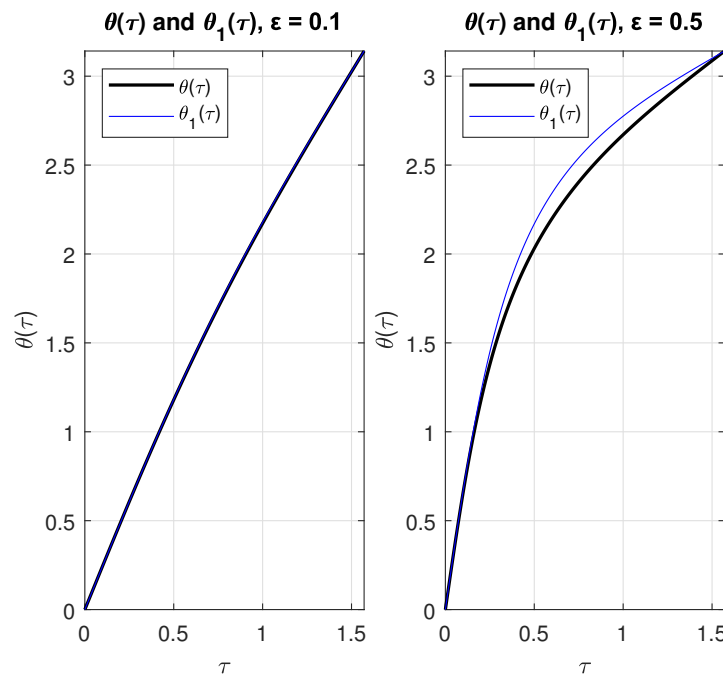


Figure 4. Plots of $\theta(\tau)$ and $\theta_1(\tau)$ with $\varepsilon = 0.1$ (left) and $\varepsilon = 0.5$ (right).

In Figure 4 we observe an evident improvement of the $\theta_1(\tau)$ approximation compared to $\theta_0(\tau)$ shown in Figure 3.

2.4. Step 3

We introduce a new function, $\psi_1(\tau)$, defined on the open interval $\tau \in (0, \frac{\pi}{2})$:

$$\psi_1(\tau) = \frac{\varphi(\tau)}{\varphi_1(\tau)}. \quad (22)$$

As followed from Eqs. (18), (19) and (20):

$$\lim_{\tau \rightarrow 0} \psi_1(\tau) = 1, \quad (23)$$

$$\lim_{\tau \rightarrow \frac{\pi}{2}} \psi_1(\tau) = 1 - \varepsilon^2. \quad (24)$$

Figure 5 shows the plot of $\psi_1(\tau)$ with ε as parameter.

We introduce the function $\varphi_2(\tau)$ as follows:

$$\varphi_2(\tau) = \psi_1(\tau) \varphi_1(\tau) = \psi_1(\tau) \frac{\sqrt{1+\varepsilon}}{(1-\varepsilon)^{\frac{3}{2}}} \tan \tau. \quad (25)$$

The definition of $\varphi_2(\tau)$ as the product of $\psi_1(\tau)$ and $\varphi_1(\tau)$ leads us to an apparent logical paradox, since, as it follows from Eq. (22), $\varphi_2(\tau) = \varphi(\tau)$. The solution to this paradox is the fact that $\psi_1(\tau)$ is an

unknown function, which we are trying to approximate with the best precision possible. The existence of such a function is obvious, for it can be theoretically constructed point-wise. However, in this work we are looking for a quasi-analytic expression for $\psi_1(\tau)$, since the exact analytic expression for it, in principle, may not even exist.

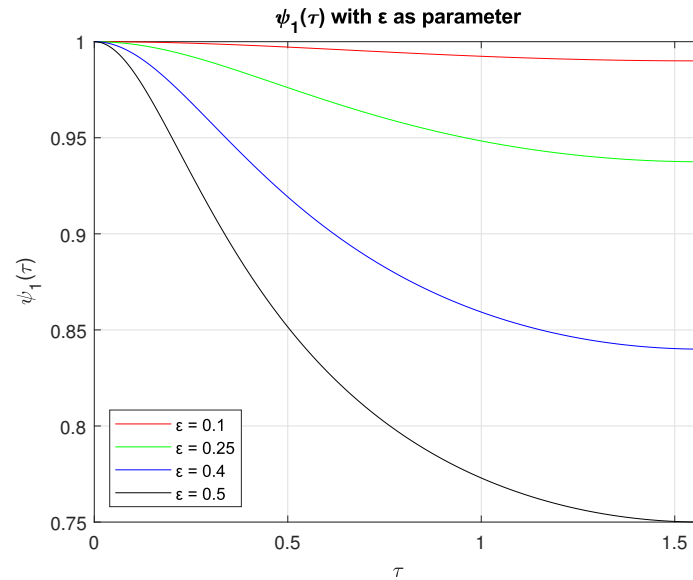


Figure 5. Plot of $\psi_1(\tau)$ with ε as parameter.

Now, we define the approximation two, $\theta_2(\tau)$ as follows:

$$\theta_2(\tau) = \begin{cases} 2 \arctan[\varphi_2(\tau)] = 2 \arctan\left(\psi_1(\tau) \frac{\sqrt{1+\varepsilon}}{(1-\varepsilon)^{\frac{3}{2}}} \tan \tau\right), \tau \in (0, \frac{\pi}{2}), \\ 0, \tau = 0, \\ \pi, \tau = \frac{\pi}{2}. \end{cases} \quad (26)$$

It should be noted that the approximation $\theta_1(\tau)$ (Eq. (21)) can be considered as the approximation $\theta_2(\tau)$ with $\psi_1(\tau) = 1$. For small values of ε , such as Earth's ($\varepsilon = 0.0167$) $\psi_1(\tau)$ has a small range (for the Earth, it will be of $[0.9997, 1]$) so that the approximation $\psi_1(\tau) = 1$ already gives us an acceptable result for certain applications. Thus, for the Earth, the maximum error of $\theta_1(\tau)$ is of 1.8×10^{-4} rad, which, translated to the error in the position, taking into account the average distance from the Earth to the Sun as 1.5×10^8 km, is equivalent to 27,000 km, which is a little more than two diameters of the Earth. Now, approximating $\psi_1(\tau)$ in a linear form, and, as a cosine with period π and amplitude adjusted to the range $[1 - \varepsilon^2, 1]$ the following corresponding approximations are obtained:

$$\theta_{2.1}(\tau) = \begin{cases} 2 \arctan\left[\left(1 - \frac{2\varepsilon^2}{\pi} \tau\right) \frac{\sqrt{1+\varepsilon}}{(1-\varepsilon)^{\frac{3}{2}}} \tan \tau\right], \tau \in [0, \frac{\pi}{2}), \\ \pi, \tau = \frac{\pi}{2}, \end{cases} \quad (27)$$

$$\theta_{2.2}(\tau) = \begin{cases} 2 \arctan\left[\left(1 + \frac{\varepsilon^2}{2}(\cos 2\tau - 1)\right) \frac{\sqrt{1+\varepsilon}}{(1-\varepsilon)^{\frac{3}{2}}} \tan \tau\right], \tau \in [0, \frac{\pi}{2}), \\ \pi, \tau = \frac{\pi}{2}. \end{cases} \quad (28)$$

The approximation $\theta_{2.1}(\tau)$ gives a maximum error of 2.24×10^{-5} rad, which translates to 3400 km in the position (slightly more than half the Earth's radius), and the approximation $\theta_{2.2}(\tau)$ gives a maximum error of 3.11×10^{-6} rad, which corresponds to approximately 470 km in the position.

In Figure 5, we notice that the shape of the curves resembles an arctangent function, with a mapping of the argument from $(-\infty, \infty)$ to $(\frac{\pi}{2}, 0)$, with the range mapping from $(-\frac{\pi}{2}, \frac{\pi}{2})$ to $(1 - \varepsilon^2, 1)$, and with the behavior of the argument being asymmetric and nonlinear. By the aforementioned, we search for the approximation of the function $\psi_1(\tau)$ in the following form:

$$\psi_1(\tau) = 1 + \frac{\varepsilon^2}{2} \left(\frac{2}{\pi} \arctan[\xi(\varepsilon, \tau)] - 1 \right), \quad (29)$$

where:

$$\xi(\varepsilon, \tau) = a_1 \tau^{-2} + a_2 \tau^{-1} + a_3 \tau + b_1 \left(\tau - \frac{\pi}{2} \right)^{-2} + b_2 \left(\tau - \frac{\pi}{2} \right)^{-1} + b_3 \left(\tau - \frac{\pi}{2} \right), \quad (30)$$

with a_i y b_i ($i = 1, 2, 3$) being functions of ε .

In order to evaluate the coefficients a_i and b_i (the six numerical coefficients mentioned in the introduction), two methods were developed, *Method A* and *Method B*. In *Method A*, the coefficients are calculated for each value of ε , while in *Method B*, they are expressed as analytic functions which, in turn, depend on other numeric coefficients, that are calculated for ranges of ε . As will be seen further, *Method A* is more accurate, but less general, while *Method B* is slightly less accurate (especially after a certain value of ε), but more general and easier to use in applications.

2.4.1. Method A

The coefficients $a_i(\varepsilon)$ and $b_i(\varepsilon)$ were calculated numerically for each eccentricity value, corresponding to every planet of the solar system, by means of RMSE (Root Mean Square Error) minimization, using MATLAB 2020b.

Figure 6 shows the behavior of $a_i(\varepsilon)$ and $b_i(\varepsilon)$ in the range of $\varepsilon \in (0, 0.5)$ (this range was selected because some absolute values of $a_i(\varepsilon)$ and $b_i(\varepsilon)$ grow drastically after $\varepsilon = 0.5$, which does not allow us to appreciate the behavior before $\varepsilon = 0.5$).

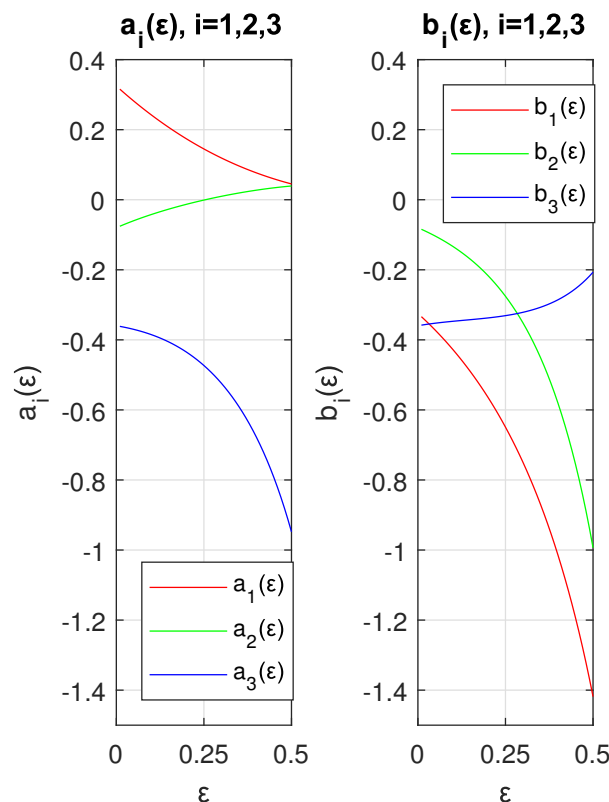


Figure 6. Plots of $a_i(\varepsilon)$ (left) and $b_i(\varepsilon)$ (right).

Table 1 shows the values of $a_i(\varepsilon)$ and $b_i(\varepsilon)$, as well as the error of $\theta(\tau)$ for the Earth and Pluto, in radians, where ME is the Maximum absolute Error, MAE is the Mean Absolute Error and RMSE is the Root Mean Square Error.

Table 1. Values of a_i and b_i and error in $\theta(\tau)$ for the Earth and Pluto.

Planet	ε	a_1	a_2	a_3	b_1	b_2	b_3	ME	MAE	RMSE
Earth	0.0167	0.310	-0.073	-0.363	-0.340	-0.087	-0.357	6.1×10^{-9}	2.9×10^{-9}	3.4×10^{-9}
Pluto	0.2488	0.146	-0.001	-0.472	-0.647	-0.274	-0.331	6.6×10^{-6}	2.8×10^{-6}	3.4×10^{-6}

Since Table 1 serves just for illustrative purposes, the values of $a_i(\varepsilon)$ and $b_i(\varepsilon)$ were rounded to three decimal places. A detailed table including more accurate values for all planets will be shown in the section of Results. For now let us mention that the absolute maximum error in the position of the Earth is 915 meters and approximately 39,000 kilometers (close to the value of the circumference of the Earth, or 16 Pluto diameters) for the position of Pluto (the average distance of Pluto to the Sun is approximately 5.9 billion kilometers).

2.4.2. Method B

Analyzing Figure 6, it can be seen that the shapes of the curves have a behavior of a cubic polynomial, so we search for the coefficients $a_i(\varepsilon)$ and $b_i(\varepsilon)$ in the following form:

$$\begin{aligned} a_i(\varepsilon) &= a_{ij}\varepsilon^j, \\ b_i(\varepsilon) &= b_{ij}\varepsilon^j, \\ i &= 1, 2, 3, \\ j &= 0, 1, 2, 3, \end{aligned} \quad (31)$$

where repeated indices imply summation.

We introduce the approximation $\theta_3(\tau)$ with the same form of $\theta_2(\tau)$ given by Eqs. (26), (29), (30), where now Eq. (31) is used to approximate the a_i and b_i in Eq. (30).

The attempt to calculate the coefficients a_{ij} and b_{ij} in the complete range of $\varepsilon \in (0,1)$ was not successful. Thus, it was decided to divide the range into five intervals, $\varepsilon \in (0,0.1]$, $\varepsilon \in (0.1,0.25]$, $\varepsilon \in (0.25,0.5]$, $\varepsilon \in (0.5,0.7]$ and $\varepsilon \in (0.7,1)$. In the next section, we will present the values of a_{ij} and b_{ij} by ranges, and compare the precision of the approximation $\theta_2(\tau)$, which uses values of $\psi_1(\tau)$ calculated using *Method A*, with that of $\theta_3(\tau)$.

3. Results

We now compare the results of our quasi-analytical solution with the real orbits of the planets of the solar system. First, we resume the results obtained above in the following equations. By the change of variable:

$$\tau = \frac{1}{\alpha^2 \mu} \frac{(1 - \varepsilon^2)^{\frac{3}{2}}}{2} t, \quad (32)$$

the equations of motion in the polar coordinate system with the origin at the Sun, and in the interval of time $\tau \in [0, \frac{\pi}{2}]$ ($t \in [0, \frac{T}{2}]$), $\theta \in [0, \pi]$ are the following:

$$\theta(\tau) = \begin{cases} 2 \arctan \left[\left(1 + \frac{\varepsilon^2}{2} \left(\frac{2}{\pi} \arctan[\tilde{\zeta}(\varepsilon, \tau)] - 1 \right) \right) \frac{\sqrt{1+\varepsilon}}{(1-\varepsilon)^{\frac{3}{2}}} \tan \tau \right], & \tau \in (0, \frac{\pi}{2}), \\ 0, & \tau = 0, \\ \pi, & \tau = \frac{\pi}{2}, \end{cases} \quad (33)$$

$$r(\tau) = \frac{\alpha}{1 + \varepsilon \cos \theta(\tau)}, \tag{34}$$

where $\zeta(\varepsilon, \tau)$ is given by the following expression:

$$\zeta(\varepsilon, \tau) = a_1\tau^{-2} + a_2\tau^{-1} + a_3\tau + b_1\left(\tau - \frac{\pi}{2}\right)^{-2} + b_2\left(\tau - \frac{\pi}{2}\right)^{-1} + b_3\left(\tau - \frac{\pi}{2}\right), \tag{35}$$

being a_i and b_i ($i = 1, 2, 3$) functions of ε . In what follows we present the two methods developed for the calculation of the coefficients a_i and b_i .

3.1. Method A

As mentioned above, in this method, the values of a_i and b_i were calculated for each eccentricity by means of RMSE minimization in MATLAB 2020b. Table 2 shows the values of a_i and b_i , ME, MAE, and RMSE errors in $\theta(\tau)$, in radians, D_s being the average distance of the planet to the Sun in kilometers and E_p is the maximum error of the position in kilometers with respect to the real orbit.

Table 2. Values of a_i and b_i , errors in $\theta(\tau)$ and absolute position.

	Mercury	Venus	Earth	Mars	Jupiter	Saturn	Uranus	Neptune	Pluto
ε	0.2056	0.0067	0.0167	0.0935	0.0489	0.0565	0.0457	0.0113	0.2488
a_1	0.17053517	0.31862395	0.30977503	0.24694331	0.28234256	0.27609996	0.28499728	0.31453377	0.14561949
a_2	-0.01166110	-0.07705003	-0.0728542	-0.04432541	-0.06014655	-0.05731287	-0.06135776	-0.07510434	-0.0012376
a_3	-0.43861374	-0.36086494	-0.36274460	-0.38289299	-0.36985666	-0.37179675	-0.36907139	-0.36171170	-0.47217706
b_1	-0.57282655	-0.33074668	-0.34005421	-0.42023391	-0.37170483	-0.37957121	-0.36843946	-0.33499871	-0.64694223
b_2	-0.22240872	-0.08288098	-0.08742593	-0.12920751	-0.10334339	-0.10741403	-0.10166725	-0.08494978	-0.27396065
b_3	-0.33681377	-0.35855961	-0.35697508	-0.34764211	-0.35253989	-0.35161930	-0.35294044	-0.35781706	-0.33108759
ME	3.6×10^{-6}	9.5×10^{-10}	6.1×10^{-9}	3.5×10^{-7}	6.6×10^{-8}	9.4×10^{-8}	5.6×10^{-8}	2.7×10^{-9}	6.6×10^{-6}
MAE	1.5×10^{-6}	4.5×10^{-10}	2.9×10^{-9}	1.5×10^{-7}	2.9×10^{-8}	4.1×10^{-8}	2.5×10^{-8}	1.3×10^{-9}	2.8×10^{-6}
RMSE	1.9×10^{-6}	5.3×10^{-10}	3.4×10^{-9}	1.8×10^{-7}	3.5×10^{-8}	5.0×10^{-8}	3.0×10^{-8}	1.5×10^{-9}	3.4×10^{-6}
D_s	5.8×10^7	1.1×10^8	1.5×10^8	2.3×10^8	7.9×10^8	1.4×10^9	2.9×10^9	4.5×10^9	5.9×10^9
E_p	208	0.11	0.92	80	52	131	163	12	39,000

The results of Table 2 show that for small values of ε , the accuracy is high. However, for values of $\varepsilon \sim 0.25$ the error increases significantly.

3.2. Method B

As was pointed out before, in this method we calculate the coefficients of a third-degree polynomial (Eq. (31)) by minimizing the RMSE, for the ranges of ε . So, in this case, it is not necessary to calculate the a_i and b_i for each value of the eccentricity. Table 3 shows the values of the coefficients a_{ij} and b_{ij} for the different ranges of ε . Obviously, using this method results in errors greater than those of Method A.

Figure 7 shows the comparison of the errors between methods A and B. As can be seen, the error in Method B is slightly higher (especially for ME) up to values of $\varepsilon = 0.8$. For values of $\varepsilon > 0.8$ the errors of Method B increase significantly with respect to those of Method A.

Table 3. Values of a_{ij} and b_{ij} calculated in ranges of ϵ .

Range of ϵ	(0,0.1]	(0.1,0.25]	(0.25,0.5]	(0.5,0.7]	(0.7,1.0)
a_{10}	0.32464090	0.32455984	0.32493519	0.33117795	0.34799892
a_{11}	-0.90342437	-0.90136299	-0.90443788	-0.94434644	-1.02378174
a_{12}	0.79798292	0.77956682	0.78688870	0.87179816	0.99672027
a_{13}	-0.24897861	-0.19074605	-0.19470806	-0.25486105	-0.32027157
a_{20}	-0.07992819	-0.07920359	-0.07197522	-0.06646582	-0.11098658
a_{21}	0.43404410	0.41648507	0.33665965	0.29615322	0.50088661
a_{22}	-0.64017363	-0.49188569	-0.19208276	-0.09396227	-0.40748236
a_{23}	0.75341116	0.31132787	-0.07256170	-0.15093252	0.00894242
a_{30}	-0.35968044	-0.35742442	-0.15675162	6.29837377	154.50791377
a_{31}	-0.17220655	-0.22278632	-2.20357719	-41.92862343	-715.24316797
a_{32}	-0.64666864	-0.26055305	6.28024901	87.40520959	1105.82612363
a_{33}	-1.78408496	-2.80408480	-10.06884121	-65.08749455	-577.96129585
b_{10}	-0.32463507	-0.32142203	-0.09294215	6.21933680	138.39317241
b_{11}	-0.90434048	-0.97722350	-3.24616805	-42.18802414	-643.15766068
b_{12}	-1.11071449	-0.54525397	7.00356134	86.74796714	996.53861794
b_{13}	-1.63153199	-3.15712303	-11.61829996	-65.86504267	-524.44755555
b_{20}	-0.07992299	-0.07527391	0.29080466	11.97863173	287.23614950
b_{21}	-0.43571269	-0.54094614	-4.16198706	-76.07319110	-1326.12648115
b_{22}	-0.78063318	0.03353877	12.02291626	158.84151291	2048.91985911
b_{23}	-2.10660888	-4.29567159	-17.65734989	-117.20310761	-1068.68369232
b_{30}	-0.35968350	-0.36025835	-0.44346730	-3.54853992	-81.17535211
b_{31}	0.17171182	0.18402819	0.99888552	20.06864682	372.42195877
b_{32}	-0.59524043	-0.68312683	-3.34688052	-42.20159066	-574.67488149
b_{33}	1.45594036	1.66666199	4.58818969	30.87266047	298.77577747

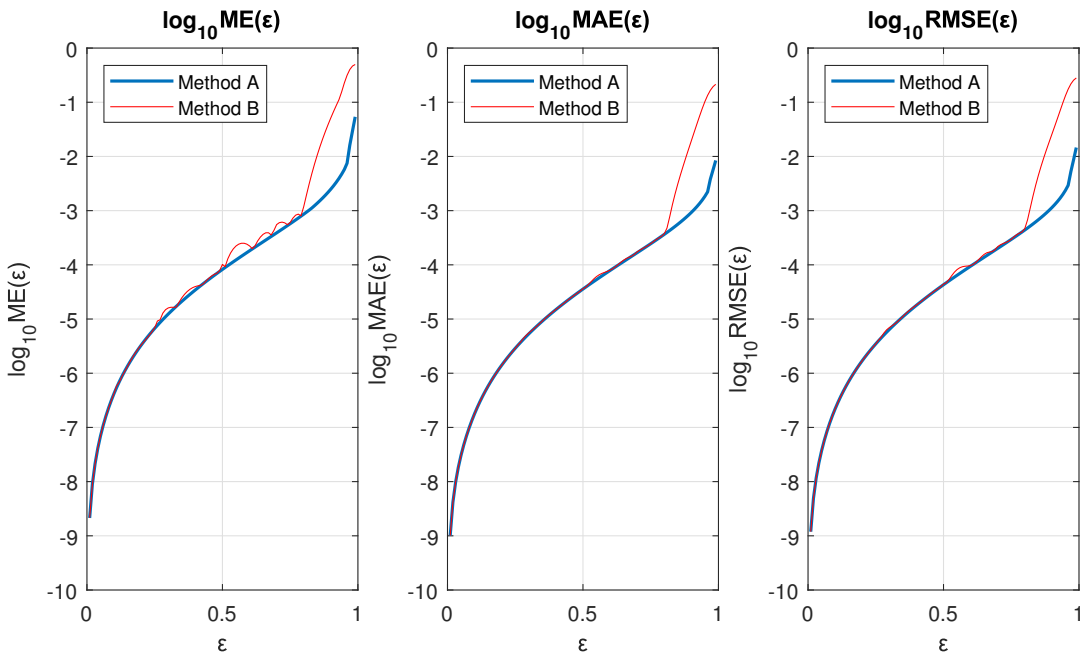


Figure 7. Logarithmic plots of the error in $\theta(\tau)$ as a function of ϵ for both methods.

3.3. Equations of Motion for the Planets

Finally, let us express the equations of motion of both position and velocity in the Cartesian coordinate system, with the origin at the Sun.

The equations for the position are:

$$\begin{aligned}x(\tau) &= r(\tau) \cos \theta(\tau), \\y(\tau) &= r(\tau) \sin \theta(\tau),\end{aligned}$$

(36)

where $\theta(\tau)$ and $r(\tau)$ are given by Eqs. (33) and (34), respectively.

The equations for the velocity are:

$$\begin{aligned} v_x &= \dot{r}(\tau) \cos \theta(\tau) - r\dot{\theta}(\tau) \sin \theta(\tau), \\ v_y &= \dot{r}(\tau) \sin \theta(\tau) + r\dot{\theta}(\tau) \cos \theta(\tau), \end{aligned} \quad (37)$$

where:

$$\begin{aligned} \dot{\theta}(\tau) &= 2 \frac{\sqrt{1+\varepsilon}}{(1-\varepsilon)^{\frac{3}{2}}} \frac{\dot{\psi}(\tau) \tan \tau + \psi(\tau) \sec^2 \tau}{1 + \frac{1+\varepsilon}{(1-\varepsilon)^3} \psi^2(\tau) \tan^2 \tau}, \\ \dot{r}(\tau) &= \frac{\alpha \varepsilon \dot{\theta}(\tau) \sin \theta(\tau)}{(1 + \varepsilon \cos \theta(\tau))^2}, \end{aligned} \quad (38)$$

and

$$\psi(\tau) = \begin{cases} 1 + \frac{\varepsilon^2}{2} \left(\frac{2}{\pi} \arctan[\zeta(\varepsilon, \tau)] - 1 \right), & \tau \in (0, \frac{\pi}{2}), \\ 1, & \tau = 0, \\ 1 - \varepsilon^2, & \tau = \frac{\pi}{2}, \end{cases} \quad (39)$$

$$\dot{\psi}(\tau) = \begin{cases} \frac{\varepsilon^2}{\pi} \frac{\dot{\zeta}(\tau)}{1 + \zeta^2(\tau)}, & \tau \in (0, \frac{\pi}{2}), \\ 0, & \tau = 0, \\ 0-, & \tau = \frac{\pi}{2}. \end{cases} \quad (40)$$

The function $\zeta(\tau)$ defined in the interval $\tau \in (0, \frac{\pi}{2})$ is given by Eq. (35) and its derivative is the following:

$$\dot{\zeta}(\tau) = -2a_1\tau^{-3} - a_2\tau^{-2} + a_3 - 2b_1\left(\tau - \frac{\pi}{2}\right)^{-3} - b_2\left(\tau - \frac{\pi}{2}\right)^{-2} + b_3. \quad (41)$$

Figure 8 shows the comparison plot between the real orbit, calculated numerically using Eq. (7), and the orbit obtained by numerical integration of Eq. (37) (where *Method A* was used). Additionally, the velocity vectors are shown at an arbitrary scale at some points of the trajectory.

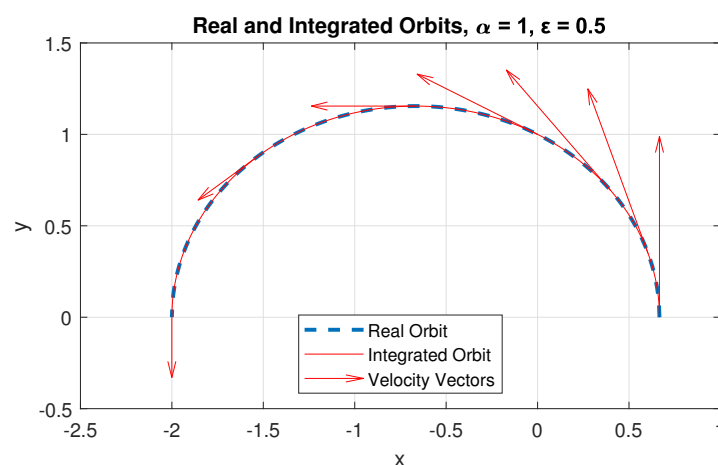


Figure 8. Plot of the orbits, real and integrated, with $\alpha = 1$ and $\varepsilon = 0.5$.

As can be seen in Figure 8, the integrated orbit closely resembles the behavior of the real orbit. This shows that our *Method A* is sufficiently accurate even for eccentricities of the order up to $\varepsilon = 0.5$.

4. Solution to Kepler's Equation

As can be seen from Figure 1b, it is trivial to obtain the following expression, which gives the formula for E (the *eccentric anomaly*), appearing in Eq. (3) as a function of the polar coordinates (ρ, θ) with the center in the focus F . In what follows, we set the major semi-axis equal to one ($a = 1$):

$$E = \arccos(F + \rho \cos \theta), \quad (42)$$

where $F = |OF|$ (Figure 1b). As is well known from the theory of conic sections, $F = \varepsilon a = \varepsilon$, since we set $a = 1$. Thus, Eq. (42) acquires the following form:

$$E = \arccos(\varepsilon + \rho \cos \theta). \quad (43)$$

Due to the normalization $a = 1$, the expression for ρ is as follows:

$$\rho = \frac{r}{a}. \quad (44)$$

The functions $\theta(\tau)$ and $r(\tau)$ are given by our final quasi-analytical solution (Eqs. (33) and (34)).

Now, in order to obtain the final explicit expression for the solution of KE, $E(M)$, we need to express θ and ρ as functions of M (the *mean anomaly* given by Eq. (4)). So far, θ and r are functions of τ (where τ is given by Eq. (6)). Thus, by expressing τ as a function of M , θ and r automatically become functions of M . The expression for $\tau(M)$ is the following:

$$\tau(M) = \frac{M}{2}. \quad (45)$$

In order to obtain ρ as a function of M , we use Kepler's third law to express a as follows:

$$a = \left(\frac{l}{2\pi\mu\sqrt{1-\varepsilon^2}} T \right)^{\frac{1}{2}}. \quad (46)$$

The final solution to KE is given by Eq. (43), using the quasi-analytical solution for the motion given by Eqs. (33) and (34) and taking into account the relations (44), (45) and (46).

5. Remarks and Conclusions

In this work, we obtained a quasi-analytical solution for the motion of the celestial bodies as an explicit function of time in four steps. We called this solution quasi-analytical, due to dependency on some numerical coefficients, which, in turn, themselves depend on the eccentricity. We proposed two methods for evaluating these coefficients, *Method A* and *Method B*. The former gives a higher degree of accuracy, but involves calculations for each value of the eccentricity, while the latter is less accurate (especially for values of $\varepsilon > 0.8$), but more practical, since it works for ranges of the eccentricity. All of our calculations involve low computational cost, and provide a high degree of accuracy for the motion of celestial bodies. Using our results, we obtained an explicit solution to KE without the need of calculating infinite series, or using numeric iterative methods.

Author Contributions: The first two A.N. Beloïarov and V.A. Beloïarov developed the theory and worked on the redaction together with the authors, R.C. Cruz-Gómez and C.O. Monzón. J.L. Romero collaborated in the theoretical revision of the manuscript.

Funding: This research received no external funding.

Informed Consent Statement: Not applicable.

Conflicts of Interest: The authors declare no conflicts of interest.

Appendix A. Integration of Eq. (1)

To solve the integral, we propose the Weierstrass change of variable:

$$u = \tan \frac{\varphi}{2}. \quad (1.1)$$

From Eq. (1.1) it follows that:

$$\cos \varphi = \frac{1 - u^2}{1 + u^2}, d\varphi = \frac{2 du}{1 + u^2}. \quad (1.2)$$

Substituting Eq. (1.2) into Eq. (1), and with a little algebra, we obtain the following:

$$F(\varphi) = \frac{2\alpha^2 \mu}{l} \int \frac{1 + u^2}{a + bu^2} du, \quad (1.3)$$

which will be left undefined for now, and will eventually be evaluated in the original variables. Here $a = 1 + \varepsilon$ and $b = 1 - \varepsilon$. To facilitate the integration, the integrand is simplified using partial fractions, leaving the integral as follows:

$$F(\varphi) = \frac{2\alpha^2 \mu}{l} \left[\frac{b-a}{b} \int \frac{du}{(a+bu^2)^2} + \frac{1}{b} \int \frac{du}{a+bu^2} \right]. \quad (1.4)$$

Doing a bit of algebra, and making the trigonometric substitution

$$\begin{aligned} u &= c \tan v, \\ du &= c \sec^2 v dv, \end{aligned}$$

where $c^2 = \frac{a}{b}$. Finally, Eq. (1.4) reads:

$$F(\varphi) = \frac{2\alpha^2 \mu}{l} \left[\frac{b-a}{b^3} \int \frac{c \sec^2 v dv}{c^4 \sec^4 v} + \frac{1}{b^2} \int \frac{c \sec^2 v dv}{c^2 \sec^2 v} \right] = \frac{2\alpha^2 \mu}{l} \left[\frac{b-a}{b^3 c^3} \int \cos^2 v dv + \frac{1}{b^2 c} \int dv \right]. \quad (1.5)$$

The latter integral is trivial, and the former is solved using the identity $\cos^2 v = \frac{1}{2}(1 + \cos 2v)$, such that $F(\varphi)$ is left as:

$$F(\varphi) = \frac{2\alpha^2 \mu}{l} \left[\left(\frac{b-a+2bc^2}{2b^3 c^3} \right) v + \frac{b-a}{2b^3 c^3} \sin v \cos v \right]. \quad (1.6)$$

Returning to the variable u , recalling that $c^2 = \frac{a}{b}$ and doing some algebra, Eq. (1.6) reads:

$$F(\varphi) = \frac{\alpha^2 \mu}{l} \left[\frac{a+b}{(ab)^{\frac{3}{2}}} \arctan \left(\sqrt{\frac{b}{a}} u \right) + \frac{b-a}{ab} \frac{u}{a+bu^2} \right]. \quad (1.7)$$

Finally, recalling Eq. (1.1), expressing a and b in terms of ε , doing algebra, and evaluating the limits of integration, we arrive at our final result:

$$t(\theta) = \frac{\alpha^2 \mu}{l} \left[\frac{2}{(1-\varepsilon^2)^{\frac{3}{2}}} \arctan \left(\sqrt{\frac{1-\varepsilon}{1+\varepsilon}} \tan \frac{\theta}{2} \right) - \frac{2\varepsilon}{1-\varepsilon^2} \frac{\tan \frac{\theta}{2}}{1+\varepsilon+(1-\varepsilon) \tan^2 \frac{\theta}{2}} \right], \quad (A1)$$

which is in agreement with Eq. (5).

Appendix B. Proofs of limits Eq. (18) and Eq. (19)

We begin by solving for $\varphi(\tau)$ from Eq. (14):

$$\varphi(\tau) = \tan \frac{\theta}{2}. \quad (2.1)$$

Next, in Eq. (15), we substitute τ by the expression Eq. (7):

$$\varphi_0(\tau) = \sqrt{\frac{1+\varepsilon}{1-\varepsilon}} \tan \left[\arctan \left(\sqrt{\frac{1-\varepsilon}{1+\varepsilon}} \tan \frac{\theta}{2} \right) - \varepsilon \sqrt{1-\varepsilon^2} \frac{\tan \frac{\theta}{2}}{1+\varepsilon+(1-\varepsilon)\tan^2 \frac{\theta}{2}} \right]. \quad (2.2)$$

We introduce the variable β as follows:

$$\beta = \tan \frac{\theta}{2}. \quad (2.3)$$

For the sake of ease, we will evaluate the limit $\frac{\varphi_0(\tau)}{\varphi(\tau)}$ instead of $\frac{\varphi(\tau)}{\varphi_0(\tau)}$.

In order to prove limit Eq. (18), we will use the Taylor expansion about zero of the following functions:

$$\begin{aligned} \tan x &= x + o(x), \\ \arctan x &= x + o(x). \end{aligned} \quad (2.4)$$

Using Eq. (2.4), we obtain:

$$\begin{aligned} \lim_{\tau \rightarrow 0} \frac{\varphi_0(\tau)}{\varphi(\tau)} &= \lim_{\beta \rightarrow 0} \frac{\varphi_0(\beta)}{\varphi(\beta)} = \lim_{\beta \rightarrow 0} \frac{1}{\beta} \sqrt{\frac{1+\varepsilon}{1-\varepsilon}} \tan \left(\sqrt{\frac{1-\varepsilon}{1+\varepsilon}} \beta - \frac{\varepsilon \sqrt{1-\varepsilon^2} \beta}{1+\varepsilon+(1-\varepsilon)\beta^2} + o(\beta) \right) = \\ &= \lim_{\beta \rightarrow 0} \frac{1}{\beta} \sqrt{\frac{1+\varepsilon}{1-\varepsilon}} \left(\sqrt{\frac{1-\varepsilon}{1+\varepsilon}} \beta - \frac{\varepsilon \sqrt{1-\varepsilon^2} \beta}{1+\varepsilon+o(\beta)} + o(\beta) \right) = \\ &= \lim_{\beta \rightarrow 0} \frac{1}{\beta} \sqrt{\frac{1+\varepsilon}{1-\varepsilon}} \beta \left(\sqrt{\frac{1-\varepsilon}{1+\varepsilon}} - \frac{\varepsilon \sqrt{1-\varepsilon^2}}{1+\varepsilon} + O(\beta) \right) = \lim_{\beta \rightarrow 0} [(1-\varepsilon+O(\beta))] = 1-\varepsilon, \end{aligned}$$

which is equivalent to:

$$\lim_{\tau \rightarrow 0} \frac{\varphi(\tau)}{\varphi_0(\tau)} = \frac{1}{1-\varepsilon}, \quad (2.5)$$

which agrees with Eq. (18).

In order to demonstrate Eq. (19), we use the following trigonometric identity:

$$\tan(a-b) = \frac{\tan a - \tan b}{1 + \tan a \tan b}. \quad (2.6)$$

Using Eq. (2.4) and Eq. (2.6), we have:

$$\begin{aligned} \lim_{\tau \rightarrow \frac{\pi}{2}} \frac{\varphi_0(\tau)}{\varphi(\tau)} &= \lim_{\beta \rightarrow \infty} \frac{\varphi_0(\beta)}{\varphi(\beta)} = \lim_{\beta \rightarrow \infty} \frac{1}{\beta} \sqrt{\frac{1+\varepsilon}{1-\varepsilon}} \tan \left[\arctan \left(\sqrt{\frac{1-\varepsilon}{1+\varepsilon}} \beta \right) - \frac{\varepsilon \sqrt{1-\varepsilon^2} \beta}{1+\varepsilon+(1-\varepsilon)\beta^2} \right] = \\ &= \lim_{\beta \rightarrow \infty} \frac{1}{\beta} \sqrt{\frac{1+\varepsilon}{1-\varepsilon}} \frac{\sqrt{\frac{1-\varepsilon}{1+\varepsilon}} \beta - \frac{\varepsilon \sqrt{1-\varepsilon^2} \beta}{1+\varepsilon+(1-\varepsilon)\beta^2} + o\left(\frac{1}{\beta}\right)}{1 + \sqrt{\frac{1-\varepsilon}{1+\varepsilon}} \frac{\varepsilon \sqrt{1-\varepsilon^2} \beta^2}{O\left(\frac{1}{\beta^2}\right) + (1-\varepsilon)\beta^2} + O\left(\frac{1}{\beta}\right)} = \\ &= \lim_{\beta \rightarrow \infty} \frac{1}{\beta} \sqrt{\frac{1+\varepsilon}{1-\varepsilon}} \frac{\sqrt{\frac{1-\varepsilon}{1+\varepsilon}} \beta + o\left(\frac{1}{\beta}\right)}{1 + \sqrt{\frac{1-\varepsilon}{1+\varepsilon}} \frac{\varepsilon \sqrt{1-\varepsilon^2}}{1-\varepsilon} + O\left(\frac{1}{\beta}\right)} = \lim_{\beta \rightarrow \infty} \frac{1 + o\left(\frac{1}{\beta}\right)}{1 + \varepsilon + O\left(\frac{1}{\beta}\right)} = \frac{1}{1+\varepsilon}, \end{aligned}$$

which is equivalent to:

$$\lim_{\tau \rightarrow \frac{\pi}{2}} \frac{\varphi(\tau)}{\varphi_0(\tau)} = 1 + \varepsilon, \quad (2.7)$$

which agrees with Eq. (19).

References

1. K. Krisciunas, Demonstrating the elliptical orbit of Mars using naked eye data, *Am. J. Phys.* (2019), DOI: 110.1119/1.5120020.
2. H. Goldstein, *Classical Mechanics, 2nd ed. Addison-Wesley, Reading.* (2020).
3. W. Baisheng, Y. Zhou, C. Lim and H. Zhong, A new solution approach via analytical approximation of the elliptic kepler equation, *Acta Astronautica* (2023), DOI: 10.1016/j.actaastro.2022.10.049.
4. P. Colwell, Solving Kepler's Equation over Three Centuries, *Willman-Bell, Inc., Richmond* (1993)
5. L. D. Landau and E. M. Lifshitz, *Mechanics, 3rd ed. Elsevier Butterworth-Heinemann, Burlington* (1976).
6. A. W. Odell and R. H. Gooding, Procedures for solving Kepler's equation, *Cel. Mech.* (1986).
7. O. González-Gaxiola and S. Hernández-Linares, An Efficient Iterative Method for Solving the Elliptical Kepler's Equation, *Int. J. Appl. Comput. Math* (2021), DOI: 10.1007/s00348-008-0556-7.
8. G. G. Elenin and T. G. Elenina, Parametrization of the Solution of the Kepler Problem and New Adaptive Numerical Methods Based on This Parametrization, *Diff Equat* (2018), DOI:10.1134/S001226611807008X.
9. F. L. Markley, Kepler Equation solver, *Celestial Mech Dyn Astr* (1995), DOI:10.1007/BF00691917.
10. A. Simha, An algebra and trigonometry-based proof of Kepler's first law, *Am. J. Phys.* (2021), DOI:10.1119/10.0005669.
11. M. Zheng, J. Luo and Z. Dang, Machine learning-based solution of Kepler's equation, *Society of Photo-Optical Instrumentation Engineers (SPIE) Conference Series* (2022), DOI:0.1117/12.2661776.
12. R. W. Easton, R. L. Anderson and M. W. Lo, Conic transfer arcs for Kepler's problem, *Am. J. Phys.* (2022), DOI:10.1119/5.0080491.
13. M. Calvo, A. Elife and L. Rández, On the integral solution of elliptic Kepler's equation, *Celest. Mech. Dyn. Astron.* (2023), DOI:10.1007/s10569-023-10142-7.
14. F. Orlando, C. Farina de Souza, C. Zarro and P. Terra, Kepler's equation and some of its pearls, *Am. J. of Phys.* (2018), DOI:10.1119/1.5055760.
15. J. B. Marion, Kepler's equation and some of its pearls, *Academic Press Inc. 1st Edition* (1965).
16. S. A. Mikkola, A cubic approximation for Kepler's equation, *Cel. Mech.* (2018), DOI:10.1007/BF01235850.

Disclaimer/Publisher's Note: The statements, opinions and data contained in all publications are solely those of the individual author(s) and contributor(s) and not of MDPI and/or the editor(s). MDPI and/or the editor(s) disclaim responsibility for any injury to people or property resulting from any ideas, methods, instructions or products referred to in the content.